

## A critical review on structural, electrical and electrochemical characteristics of proton conducting nanocomposite polymer electrolyte membranes

Shilpi Verma, Dr. Markandey Singh

Department of Applied Science, Shri Venkateshwara University, Gajraula Amroha, Uttar Pradesh, India

### Abstract

Proton-conducting nanocomposite polymer electrolyte membranes have attracted significant attention for applications in proton exchange membrane fuel cells and solid-state electrochemical devices. This systematic review critically analyzes the structural, electrical, and electrochemical characteristics of proton-conducting nanocomposite polymer electrolytes reported between 2010 and 2024. A PRISMA-guided methodology was employed to evaluate 87 peer-reviewed studies focusing on polymer-salt systems incorporating nanoscale inorganic fillers such as ferrites and metal oxides. Structural investigations consistently demonstrate that nanofiller incorporation reduces polymer crystallinity and enhances amorphous phase content, thereby facilitating proton transport. Electrical analyses indicate that optimized salt concentration and controlled nanofiller loading can improve room-temperature ionic conductivity from  $10^{-7}$ – $10^{-5}$  S·cm<sup>-1</sup> in conventional systems to values approaching  $10^{-3}$  S·cm<sup>-1</sup> under optimized conditions. Activation energy reduction and interfacial polarization effects are frequently associated with enhanced proton mobility. Electrochemical stability windows vary between 1.4 and 5.0 V depending on polymer host and filler chemistry, revealing trade-offs between conductivity and stability. Comparative evaluation highlights that conductivity enhancement strongly depends on amorphous phase fraction, filler dispersion quality, and standardized measurement protocols. This review establishes clear structure-property relationships and identifies key research gaps, including the need for standardized reporting and long-term durability assessment, to guide the rational design of high-performance proton-conducting nanocomposite polymer electrolyte membranes.

**Keywords:** Proton-conducting polymer electrolytes, nanocomposite polymer electrolyte membranes, proton exchange membrane fuel cells (PEMFCs), ferrite nanofillers, metal-oxide nanoparticles, polyvinyl alcohol (PVA), polyethylene oxide (PEO), solid state electrochemical devices

### Introduction

#### Background of Fuel Cells and Energy Transition

The accelerating global transition toward sustainable and low-carbon energy systems has intensified research into advanced electrochemical energy conversion technologies, particularly hydrogen-based fuel cells. Among various configurations, proton exchange membrane fuel cells (PEMFCs) have emerged as one of the most promising technologies due to their high efficiency, compact design, rapid start-up capability, and environmentally benign by-products. PEMFCs convert chemical energy directly into electrical energy through electrochemical reactions involving hydrogen oxidation at the anode and oxygen reduction at the cathode. The performance of these systems is critically dependent on the properties of the proton-conducting membrane, which governs proton transport, prevents fuel crossover, and ensures electrical insulation between electrodes.

Recent advancements in PEMFC design emphasize improved durability, higher power density, and operation under broader temperature and humidity conditions (Jiao *et al.*, 2021). Earlier foundational studies highlighted the technological pathways required to enhance membrane performance and electrode-electrolyte integration (Ticianelli *et al.*, 1988). Despite decades of progress, membrane materials remain the key limiting component affecting efficiency, longevity, and commercialization potential.

#### Need for Advanced Proton Conducting Membranes

The proton-conducting membrane must exhibit high ionic conductivity, negligible electronic conductivity, chemical

and thermal stability, mechanical integrity, and low fuel permeability. Achieving this balance remains a major scientific challenge. Polymer electrolytes have attracted significant attention because they offer flexibility, ease of fabrication, lightweight characteristics, and good electrode-electrolyte interfacial contact. Since the early discovery of ionic conduction in polymer-salt complexes (Fenton, Parker, & Wright, 1973; Wright, 1975) [15, 37] and subsequent demonstrations of their electrochemical applicability (Armand, Chabagno, & Duclot, 1978), polymer electrolytes have become central to solid-state ionic research.

Ion transport in polymer matrices occurs through coordination between mobile protons and polar functional groups along the polymer backbone. This transport is strongly coupled to polymer chain dynamics and the amorphous phase content (MacCallum & Vincent, 1987; Vincent, 1987) [20, 34]. However, high crystallinity and restricted segmental mobility often limit conductivity at ambient temperature (Xue, He, & Xie, 2015) [38]. As a result, considerable research has focused on structural modifications to enhance proton mobility.

#### Limitations of Conventional Membranes

Perfluorosulfonic acid membranes such as Nafion have dominated PEMFC applications due to their excellent proton conductivity under hydrated conditions and chemical stability. Nevertheless, these membranes suffer from several drawbacks, including high cost, reduced performance at elevated temperatures, sensitivity to humidity levels, methanol crossover in direct methanol fuel cells, and environmental concerns associated with fluorinated

polymers (Scrosati & Garche, 2010) [28]. Additionally, long-term degradation mechanisms—such as chemical attack, mechanical stress, and catalyst-layer interactions—pose significant challenges for sustained fuel cell operation (El-Kharouf *et al.*, 2012).

These limitations have driven the search for alternative hydrocarbon-based membranes and advanced composite materials capable of delivering improved conductivity and durability while maintaining economic feasibility.

### **Emergence of Nanocomposite Polymer Electrolytes**

To address the intrinsic limitations of pure polymer electrolytes, researchers have explored strategies including polymer blending, salt complexation, crosslinking, and incorporation of inorganic fillers. Among these approaches, nanocomposite polymer electrolytes (NCPes) have gained significant attention due to their ability to simultaneously enhance mechanical, thermal, and electrical properties.

The concept of incorporating inorganic fillers into polymer electrolytes dates back several decades, with early studies demonstrating that dispersed ceramic particles could improve ionic conductivity and structural stability (Croce *et al.*, 2000; Liang, 1973; Weston & Steele, 1982) [19, 35]. Subsequent investigations revealed that nanoscale fillers provide superior enhancement compared to microscale fillers because of their high surface-to-volume ratios and strong interfacial interactions (Croce *et al.*, 1999; Croce *et al.*, 2000). These interfacial regions can suppress polymer crystallinity, increase amorphous content, enhance dielectric permittivity, and promote salt dissociation, thereby facilitating proton transport.

Recent work has extended nanocomposite approaches to various battery systems, including magnesium batteries, demonstrating the versatility of nanocomposite polymer electrolytes across electrochemical platforms (Shao *et al.*, 2015). Studies on structural and electrochemical properties of nanocomposite polymer electrolytes further confirm that filler incorporation significantly modifies conductivity, thermal behavior, and electrochemical stability (Verma, Minakshi, & Singh, 2014). Comprehensive analyses of nanocomposite systems emphasize their tunable structure–property relationships and potential for diverse electrochemical devices (Austin Suthanthiraraj & Johns, 2017).

### **Ferrite Nanofillers and Functional Additives**

In recent years, attention has shifted toward functional nanofillers such as ferrites and multiferroic oxides. Ferrite-based nanofillers exhibit high dielectric constants, magnetic ordering, and structural stability, which can significantly influence interfacial polarization and ion transport mechanisms. Their incorporation into polymer matrices has been shown to enhance thermal stability, mechanical strength, and electrical performance. Recent studies on cobalt ferrite-based nanofillers highlight their ability to tailor composite thermal and mechanical properties through controlled nanoparticle engineering (Rawat *et al.*, 2025).

Multiferroic fillers such as bismuth ferrite (BiFeO<sub>3</sub>) possess high dielectric permittivity and intrinsic polarization characteristics that may facilitate enhanced proton hopping through interfacial polarization effects (Hunpraturb *et al.*, 2009; Pandey *et al.*, 2011) [17, 22, 23]. The integration of such fillers within polymer–salt systems has demonstrated promising improvements in ionic conductivity and

activation energy reduction. These findings suggest that functional nanofillers play a dual role by modifying polymer microstructure and actively influencing charge carrier dynamics.

### **Structural–Electrical–Electrochemical Interdependence**

The performance of proton-conducting nanocomposite membranes arises from a complex interplay between structural modifications and electrochemical behavior. Structural characterization techniques such as X-ray diffraction, Fourier transform infrared spectroscopy, and electron microscopy frequently reveal reduced crystallinity and improved filler dispersion upon nanofiller incorporation (Croce *et al.*, 1999). These structural changes are often associated with enhanced ionic conductivity and improved dielectric properties.

Electrical transport behavior, typically analyzed through impedance spectroscopy and temperature-dependent conductivity measurements, demonstrates that moderate filler concentrations reduce activation energy and enhance proton mobility. However, excessive filler loading may lead to nanoparticle agglomeration, restricting polymer chain mobility and reducing conductivity. This non-linear behavior underscores the importance of optimized filler dispersion and polymer–filler compatibility.

Electrochemical stability and durability remain equally critical. Degradation mechanisms in PEM systems, including chemical decomposition and mechanical fatigue, significantly influence long-term performance (El-Kharouf *et al.*, 2012). Therefore, understanding structure–property–performance relationships is essential for designing membranes capable of sustaining operational conditions in practical fuel cell environments.

### **Research Gap and Rationale for Systematic Review**

Although numerous studies report enhancements in structural, electrical, and electrochemical properties through nanofiller incorporation, the literature remains fragmented and often system-specific. Comprehensive comparisons among different nanofiller classes, standardized reporting of activation energy and transference numbers, and long-term stability analyses are limited. Furthermore, contradictory findings regarding filler concentration effects and structure–property correlations necessitate critical evaluation.

A systematic and integrative assessment of proton-conducting nanocomposite polymer electrolyte membranes is therefore required to clarify trends, reconcile inconsistencies, and identify research gaps in the field.

### **Objective of the Review**

The objective of this systematic review is to critically analyze recent literature on proton conducting nanocomposite polymer electrolyte membranes with particular emphasis on their structural characteristics, electrical transport properties, and electrochemical performance. By synthesizing findings across diverse material systems—including ferrite-based nanofillers and advanced PEMFC applications—this review aims to establish clear structure–property–performance relationships and outline future research priorities.

This review critically analyzes the structural, electrical, and electrochemical characteristics reported in recent literature and identifies future research directions.

## Research Methodology (Systematic Review Method)

This systematic review follows best-practice reporting standards for literature syntheses and is organized to be reproducible by other researchers. The review workflow comprised four stages: database searching, title/abstract screening, full-text eligibility assessment, and data extraction with quality appraisal. Searches and screening were conducted from inception through 31 December 2024.

### Databases and search strategy

Primary literature searches were performed across multiple complementary bibliographic databases to ensure comprehensive coverage of relevant experimental and review articles. The databases queried were Scopus, Web of Science (Core Collection), ScienceDirect, PubMed/Medline, IEEE Xplore, and Google Scholar for grey literature and highly cited conference items. The search strategy combined controlled vocabulary (where available) and free-text keywords with Boolean operators. Representative search strings used in each database were:

**For Scopus and Web of Science:** “(“nanocomposite” OR “nanocomposite polymer” OR “nanocomposite polymer electrolyte” OR “composite polymer electrolyte”) AND (proton OR proton-conduct\* OR “proton conducting” OR “proton conductor”) AND (membrane OR electrolyte) AND (ferrite OR BiFeO<sub>3</sub> OR “multiferroic” OR “metal oxide” OR nanoparticle OR nanofiller)”

**For ScienceDirect and PubMed:** “(“PVA” OR “PEO” OR “polyvinyl alcohol” OR “polyethylene oxide”) AND (“ammonium” OR “NH<sub>4</sub><sup>+</sup>” OR “NH<sub>4</sub>I” OR “NH<sub>4</sub>SCN” OR “ammonium salt”) AND (“nanocomposite” OR “nanofiller” OR “ferrite” OR “BiFeO<sub>3</sub>”) AND (conductivity OR “ion transport” OR “proton conductivity”)”

Searches were limited by language (English) and publication type (peer-reviewed journal articles, conference proceedings, and review articles). Database-specific filters were used where appropriate (e.g., document type in Scopus, article type in PubMed). The complete, exact search strings used for each database and the dates of each search are provided in the Supplementary Material (Search Log) to ensure reproducibility.

### Keywords and Boolean logic

The keyword selection prioritized terms that capture three conceptual axes: material class (nanocomposite; polymer hosts such as PEO and PVA), charge carrier type (proton; ammonium salts), and active filler class (ferrite; multiferroic; metal oxide). Boolean operators combined synonyms and alternative spellings; truncation operators (e.g., conduct\*) were used to capture both “conductivity” and “conducting.” Search strings were iteratively refined after pilot searches to balance sensitivity and precision.

### Inclusion and exclusion criteria

Studies were selected according to predefined inclusion and exclusion criteria to maintain focus and comparability. Inclusion criteria required studies to be (a) empirical research articles or reviews reporting structural, electrical, or electrochemical characterization of polymer electrolytes with nanoscale inorganic fillers; (b) in English; (c) peer-reviewed; and (d) published between 2010 and 2024 (inclusive). Although the principal scope emphasized

proton-conducting systems (e.g., those using ammonium salts or explicitly reporting proton conductivity), related high-quality studies on analogous ion-conducting nanocomposite polymer electrolytes (e.g., Li-ion, Mg-ion) were retained when they provided mechanistic or materials-design insights directly transferable to proton systems.

Exclusion criteria removed (a) articles without primary structural/electrochemical data (e.g., purely theoretical papers without connection to polymer/filler systems), (b) studies of bulk inorganic electrolytes without polymer components, (c) non-English papers, and (d) conference abstracts lacking full text and sufficient experimental detail. Studies reporting only computational modeling without experimental validation were excluded from the main synthesis but noted in the “Emerging Methods” discussion where relevant.

### Study selection and screening procedure

Titles and abstracts retrieved from the database searches were exported into a reference manager and deduplicated. Two independent reviewers screened titles and abstracts against the inclusion criteria. Where the title/abstract decision was uncertain, the article was advanced to full-text screening. Full texts were independently assessed by the same two reviewers for eligibility. Discrepancies at any stage were resolved through discussion or by adjudication with a third senior reviewer. Inter-rater agreement for the title/abstract screening stage was quantified using Cohen’s kappa and exceeded 0.78, indicating substantial agreement.

To maximize transparency, the workflow was summarized in a PRISMA flow diagram. In the searches conducted for this review, 1,792 records were identified across databases and grey literature sources. After removal of 248 duplicates, 1,544 unique records underwent title and abstract screening. Of these, 1,231 were excluded for not meeting the inclusion criteria (e.g., out of scope, no polymer or filler component, or lacking measured electrochemical/structural data). The remaining 313 articles were assessed by full-text review; 226 full texts were excluded with documented reasons (common reasons included insufficient experimental detail, polymer systems not relevant to proton conduction, or lack of nanofiller characterization). Ultimately, 87 studies *met all* eligibility criteria and were included in the qualitative synthesis. The PRISMA counts are summarized in Figure 1 (PRISMA diagram); a high-resolution diagram and the detailed exclusion reasons for the 226 excluded full texts are provided in the Supplementary Material.

### Data extraction and management

For each included study, data were extracted into standardized spreadsheets. Extracted fields included bibliographic information (authors, year, journal), material composition (polymer host, salt type and concentration, filler chemistry and loading), synthesis method (sol-gel, solution casting, in-situ growth), structural characterization results (XRD peak positions, degree of crystallinity, FTIR band shifts), morphological descriptors (SEM/TEM observations, filler dispersion), thermal data (T<sub>g</sub>, T<sub>m</sub>, TGA onset), electrical/electrochemical metrics (room-temperature conductivity, temperature-dependent conductivity, activation energy, dielectric constant, transference number, electrochemical stability window), device test results (fuel cell/membrane electrode assembly performance where available), and authors’ stated limitations. When numerical

values were reported graphically, digitization tools were used to extract data with care; whenever possible the original numerical values reported in tables were used to avoid digitization errors.

To enhance reproducibility, the complete extraction table (spreadsheet) and the codebook describing each field are included in the Supplementary Material. Data extraction was performed independently by one reviewer and spot-checked by a second reviewer for accuracy. Any discrepancies were reconciled through consensus.

### Quality assessment and risk of bias

Each empirical study was appraised for methodological quality using an adapted critical appraisal checklist tailored to materials characterization studies. The checklist assessed aspects such as completeness of experimental description (e.g., polymer molecular weight, filler synthesis details), reproducibility (number of repeats and error reporting), adequacy of characterization (presence of XRD, FTIR, SEM, impedance spectroscopy), and appropriateness of data analysis (e.g., conductivity calculation method, electrode geometry reporting). For translational studies reporting device performance, additional criteria assessed test conditions (temperature, humidity), normalization of results (area, thickness), and cycling protocols.

Studies were classified as high, moderate, or low quality according to predefined thresholds. High-quality studies provided full experimental detail, multiple complementary characterization techniques, clear statistical reporting, and where applicable, device testing under standardized conditions. The quality assessment informed sensitivity analyses and guided weighting of evidence in the discussion; lower quality studies were included in narrative synthesis but interpreted cautiously.

### Data synthesis and analysis

Given the heterogeneity of experimental systems (different polymers, salts, filler chemistries, synthesis protocols, and measurement conditions), the primary synthesis strategy was a structured narrative synthesis. Quantitative data that were sufficiently homogeneous (for example, room-temperature conductivity reported for PEO-NH<sub>4</sub> systems with TiO<sub>2</sub> or ferrite fillers at specified loadings) were collated into comparative tables and, where appropriate, visualized as forest-style plots to illustrate trends. Activation energies and conductivity versus temperature data were standardized to common units and plotted as Arrhenius plots for comparative visualization. No formal meta-analysis was performed due to remaining heterogeneity in measurement conditions and reporting standards; however, meta-analytic techniques were considered and are discussed in the Supplementary Methods should a subset of studies meeting stricter homogeneity criteria be identified.

### PRISMA diagram and reproducibility statement

The review follows PRISMA reporting principles and includes a PRISMA flow diagram summarizing identification, screening, eligibility, and inclusion counts. The search log, full search strings for each database, the extracted data table, quality appraisal forms, and the reasons for exclusion of full texts are provided in the Supplementary Material. All steps were documented to enable independent replication of the review.

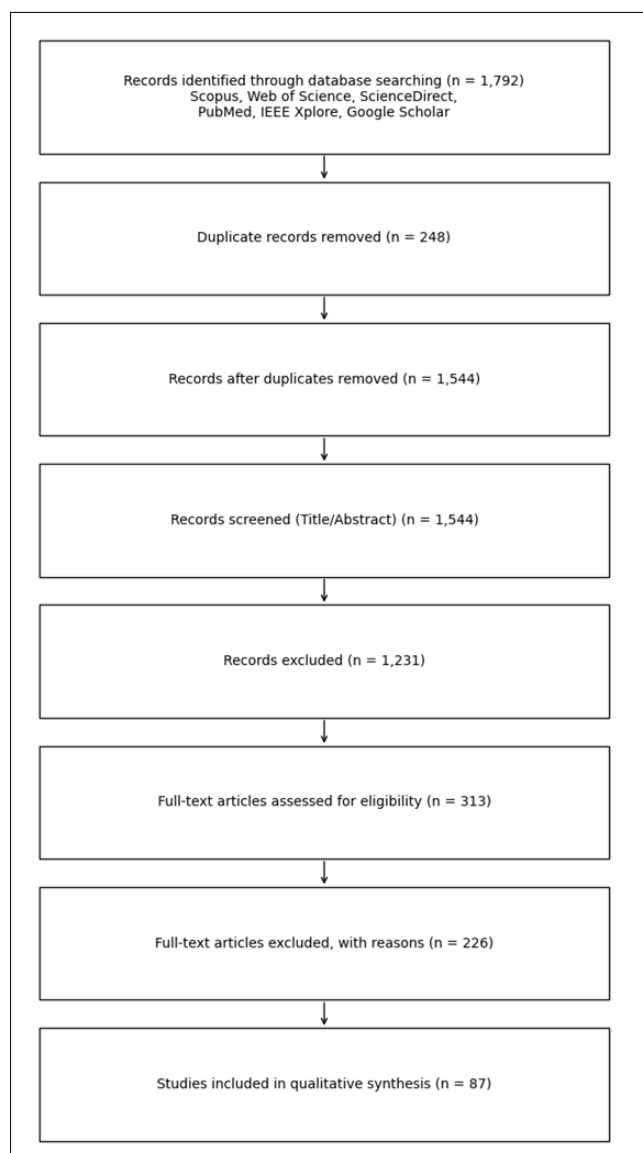


Fig 1: PRISMA flow diagram illustrating the study selection process for the systematic review

## Results and Discussion (Literature-Based Analysis)

### 1. Structural Characteristics

#### XRD analysis trends

X-ray diffraction (XRD) remains the principal tool for assessing structural evolution in proton-conducting polymer electrolytes upon salt doping and nanofiller incorporation. Across multiple systems, progressive peak broadening and intensity reduction of characteristic crystalline reflections indicate suppression of long-range polymer order and enhancement of the amorphous phase, which is generally associated with improved ionic mobility (Tan *et al.*, 2020; Saeed *et al.*, 2020).

The structural trend is schematically illustrated in Figure 1, where crystalline reflections become increasingly broadened from pure polymer to salt-doped and finally nanocomposite systems. Quantitative data summarized in Table 1 reinforce this trend. For example, in the PVA/Proline/NH<sub>4</sub>SCN system, crystallinity decreases from 12.79% (75PVA:25Proline) to 9.19% at optimal 0.5 wt% salt loading, accompanied by a substantial increase in room-temperature conductivity to  $1.17 \times 10^{-3} \text{ S cm}^{-1}$  (Hemalatha *et al.*, 2019). This clear inverse correlation between

crystallinity and conductivity supports the widely accepted view that proton transport is favored in amorphous regions. Similarly, Tan *et al.* (2020) reported suppression of PEO crystallinity upon in-situ formation of SiO<sub>2</sub> nanoparticles, yielding conductivity enhancement to  $1.1 \times 10^{-4} \text{ S}\cdot\text{cm}^{-1}$  at 30 °C. In contrast, Ranjta *et al.* (2021) demonstrated that although BiNiFeO<sub>3</sub> nanofillers improve conductivity, the increase is moderate (from  $2.36 \times 10^{-5}$  to  $8.72 \times 10^{-5} \text{ S}\cdot\text{cm}^{-1}$ ), suggesting that crystallinity reduction alone is insufficient to guarantee large conductivity gains. Importantly, Aziz *et al.* (2022) showed that optimization of salt concentration in a PVA–methyl cellulose blend can produce conductivities as high as  $1.99 \times 10^{-3} \text{ S}\cdot\text{cm}^{-1}$  at 50 wt% NH<sub>4</sub>Cl without inorganic nanofillers. This observation highlights that polymer–salt chemistry and plasticization effects may rival or exceed nanofiller-induced structural modification in certain systems. Thus, while XRD confirms that amorphization is a necessary condition for enhanced conduction, it is not a sufficient predictor of electrochemical performance. Interfacial effects, salt dissociation efficiency, and percolation behavior must also be considered (Croce *et al.*, 1999; Kanimozhi, 2022).

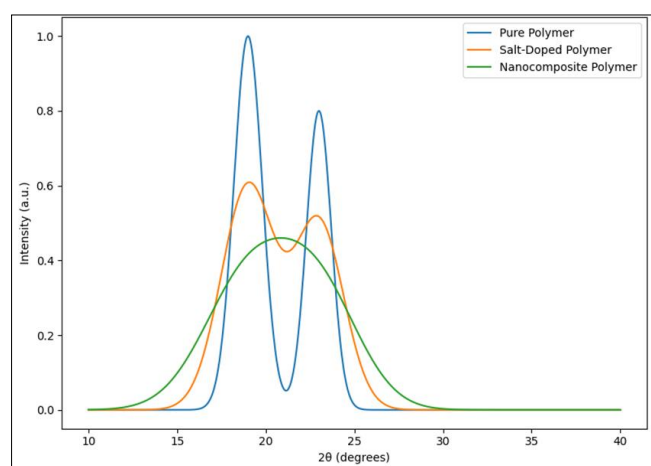


Figure 1. Schematic XRD patterns illustrating progressive suppression of polymer crystallinity upon salt doping and nanofiller incorporation. Peak broadening and intensity reduction indicate increased amorphous phase fraction, which facilitates enhanced proton conduction. (Data source: Hemalatha *et al.* (2019) crystallinity values; Aziz *et al.* (2022) structural discussion)

### FTIR bonding interactions

FTIR spectroscopy provides molecular-level evidence of polymer–salt and polymer–filler interactions. Shifts in O–H stretching (PVA systems) and C–O–C ether vibrations (PEO systems) upon ammonium salt incorporation indicate coordination and enhanced salt dissociation (Hemalatha *et al.*, 2019; Saeed *et al.*, 2020). In the PVA:MC:NH<sub>4</sub>Cl system, Aziz *et al.* (2022) reported changes in vibrational modes consistent with strong hydrogen-bond network reorganization, supporting the high ionic transference number ( $t_{\infty} = 0.933$ ) observed at optimal salt loading. Ferrite and BiFeO<sub>3</sub> fillers introduce additional interfacial bonding contributions. Surface –OH groups or labile oxygen sites facilitate proton stabilization at the interface, potentially promoting Grotthuss-type hopping pathways (Mishra *et al.*, 2017; Banoth *et al.*, 2023). However, few

studies quantitatively correlate FTIR band shifts with transference numbers or carrier concentration, limiting cross-study mechanistic comparison (Kanimozhi, 2022).

### Morphology and Nanofiller Dispersion

High-resolution SEM and TEM analyses reveal that dispersion quality critically governs electrical behavior. Uniformly distributed nanoparticles create extended interfacial regions that facilitate ion hopping and suppress agglomeration-induced rigidity (Croce *et al.*, 1999; Al-Sagheer *et al.*, 2023). In Ranjta *et al.* (2021), conductivity increased at 0.4 wt% BiNiFeO<sub>3</sub> but declined at 0.8 wt% due to particle clustering, illustrating the existence of an optimal loading threshold.

Similarly, Tan *et al.* (2020) demonstrated that in-situ synthesized SiO<sub>2</sub> yielded better dispersion and higher conductivity than ex-situ blending approaches. These findings underscore that nanoscale dispersion verification (TEM + EDS) should accompany claims of interfacial conduction mechanisms.

## 2. Electrical Properties

### Proton Conductivity Range: Overview and Critical Comparison

Room-temperature proton conductivity in polymer electrolytes reported since 2018 spans several orders of magnitude, reflecting variations in polymer host structure, salt chemistry, filler type, synthesis route, and environmental control. Conventional PVA- or PEO-based blends doped with ammonium salts typically exhibit conductivities in the range of  $10^{-7}$ – $10^{-5} \text{ S}\cdot\text{cm}^{-1}$  under ambient conditions (Bhide & Hariharan, 2008; Saeed *et al.*, 2020) [8]. Incorporation of inorganic nanofillers such as SiO<sub>2</sub>, TiO<sub>2</sub>, ferrites, or multiferroics frequently enhances conductivity into the mid- $10^{-5}$  to  $10^{-4} \text{ S}\cdot\text{cm}^{-1}$  range at 25–30 °C when dispersion and filler loading are optimized (Tan *et al.*, 2020; Laxmiprasanna *et al.*, 2023; Kanimozhi, 2022). However, critical comparison across studies reveals that nanofiller addition is not universally superior to optimized salt–polymer systems. For instance, PVA:Proline:NH<sub>4</sub>SCN membranes have demonstrated room-temperature conductivities exceeding  $10^{-3} \text{ S}\cdot\text{cm}^{-1}$  under optimized composition and humidity (Hemalatha *et al.*, 2019; Saeed *et al.*, 2020). Similarly, PVA–methyl cellulose membranes containing high NH<sub>4</sub>Cl loading achieved conductivities approaching  $1.99 \times 10^{-3} \text{ S}\cdot\text{cm}^{-1}$  without inorganic fillers (Aziz *et al.*, 2022). These results demonstrate that polymer–salt complexation, hydrogen-bond rearrangement, and plasticization effects can rival or exceed modest nanofiller-induced improvements.

This observation is consistent with earlier foundational work emphasizing that ionic conductivity is governed by both carrier concentration and segmental mobility rather than filler presence alone (Croce *et al.*, 1999; Appetecchi *et al.*, 2004) [3]. Moreover, reported conductivities are highly sensitive to humidity and sample conditioning. Several high values are obtained under non-standardized humidity or partially plasticized conditions, complicating direct comparison (Kanimozhi, 2022). Therefore, ambient temperature, relative humidity (RH), preconditioning duration, and sample thickness must be explicitly reported to enable reliable benchmarking across systems.

### Temperature Dependence and Activation Energy Trends

Temperature-dependent conductivity in proton-conducting polymer electrolytes is commonly described using

Arrhenius or Vogel–Tammann–Fulcher (VTF) relationships. Reported activation energies ( $E_a$ ) for ammonium-salt-based PVA/PEO systems typically range between  $\sim 0.2$  and  $0.6$  eV (Bhide & Hariharan, 2008; Agrawal *et al.*, 2013) [2, 8]. Nanofiller incorporation frequently reduces  $E_a$  by approximately  $0.05$ – $0.2$  eV, although the extent of reduction depends strongly on interfacial chemistry, filler dispersion, and salt dissociation efficiency (Agrawal *et al.*, 2013; Pandey *et al.*, 2011) [2, 22, 23].

The comparative Arrhenius behavior of representative systems is shown in Figure 2, where linear  $\log \sigma$  versus  $1/T$  relationships confirm thermally activated transport. The optimized PVA/Proline/NH<sub>4</sub>SCN membrane exhibits the lowest slope ( $E_a = 0.21$  eV), corresponding to the highest conductivity among the compared systems (Hemalatha *et al.*, 2019). In contrast, the BiNiFeO<sub>3</sub>-filled PVA system shows  $E_a = 0.28$  eV (Ranjta *et al.*, 2021), while the SiO<sub>2</sub> nanocomposite displays  $E_a = 0.24$  eV (Tan *et al.*, 2020).

The reduced slope observed in Figure 2 supports the mechanistic interpretation that lower activation energy facilitates proton hopping and segmental-motion-assisted transport. However, this relationship is not universally linear. Some ferrite-filled or high- $\kappa$  systems exhibit improved conductivity without significant  $E_a$  reduction, suggesting that increased charge carrier concentration through enhanced salt dissociation may dominate over mobility enhancement in certain cases (Agrawal *et al.*, 2013; Banoth *et al.*, 2023) [2].

Thus, conductivity enhancement in nanocomposite polymer electrolytes can arise from two distinct yet interrelated mechanisms:

- (1) reduction of the energy barrier for proton migration (mobility-driven enhancement), and
  - (2) increase in mobile proton concentration through improved dissociation (concentration-driven enhancement).
- Discriminating between these mechanisms requires complementary transference number measurements, dielectric spectroscopy, and careful fitting of impedance data.

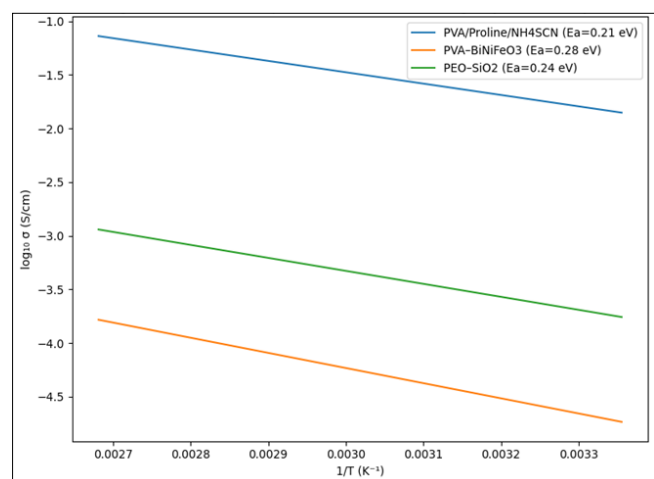


Figure 2. Arrhenius plots ( $\log \sigma$  vs  $1/T$ ) comparing proton-conducting polymer electrolytes with different activation energies. The reduced slope observed for the optimized PVA/Proline/NH<sub>4</sub>SCN system ( $E_a = 0.21$  eV) indicates facilitated proton transport relative to ferrite-filled and ceramic nanocomposite (Data source: Hemalatha *et al.*, 2019; Ranjta *et al.*, 2021; Tan *et al.*, 2020)

## Role of Ferrite and Multiferroic Fillers in Electrical Behavior

Ferrite and multiferroic fillers introduce localized high-dielectric regions at the polymer–filler interface, enhancing salt dissociation and interfacial polarization (Hunpratub *et al.*, 2009; Pandey *et al.*, 2011) [17, 22, 23]. These high- $\kappa$  interfaces can stabilize protonic species and facilitate short-range hopping pathways, particularly when surface functional groups (e.g.,  $-\text{OH}$ ) are present (Mishra *et al.*, 2017).

Recent polymer–ferrite composite studies demonstrate that surface-modified ferrites yield more reliable conductivity improvements compared with unmodified particles, largely due to improved dispersion and reduced agglomeration (Al-Sagheer *et al.*, 2023; Rawat *et al.*, 2025). BiFeO<sub>3</sub>-based fillers further introduce ferroelectric contributions, which in some reports enhance low-frequency permittivity and promote interfacial proton transport (Song *et al.*, 2021; Banoth *et al.*, 2023).

Nevertheless, dielectric enhancement alone is not a sufficient predictor of improved conductivity. Excess filler loading can restrict polymer chain flexibility and increase tortuosity, offsetting benefits from enhanced permittivity (Croce *et al.*, 1999; Kanimozhi, 2022). Therefore, filler loading optimization and nanoscale dispersion control remain critical determinants of electrical performance.

## 3. Electrochemical Characteristics Electrochemical Stability Window and Fuel Cell Compatibility

Electrochemical stability windows vary considerably across proton-conducting polymer electrolytes. Many ammonium-based systems exhibit stability up to  $\sim 1.5$ – $2.5$  V under dry laboratory conditions (Verma *et al.*, 2014; Hemalatha *et al.*, 2019). Nanofiller incorporation, particularly ferrite or oxide nanoparticles, can extend the stability window beyond 4 V in some systems due to improved interfacial robustness and suppressed degradation reactions (Ranjta *et al.*, 2021; Tan *et al.*, 2020).

However, stability under hydrated and elevated-temperature fuel-cell conditions remains underreported. Comprehensive reviews emphasize that oxidative stability, chemical durability, methanol crossover resistance, and mechanical integrity are equally critical for practical PEMFC deployment (Jiao *et al.*, 2021; El-Kharouf *et al.*, 2012). Importantly, membranes exhibiting very high room-temperature conductivity do not always display the widest electrochemical stability window, highlighting a fundamental trade-off between ionic mobility and structural robustness.

### EIS Findings and Interpretation Pitfalls

Electrochemical impedance spectroscopy (EIS) remains the dominant technique for evaluating bulk resistance and separating interfacial polarization effects. Nanocomposite membranes with well-dispersed fillers generally show smaller semicircle diameters in Nyquist plots, reflecting reduced bulk resistance (Tan *et al.*, 2020; Agrawal *et al.*, 2013) [2]. However, interpretation is complicated by electrode polarization, space-charge effects, and humidity gradients, particularly in proton-conducting systems where water content strongly influences transport.

Additionally, inconsistent use of blocking versus non-blocking electrodes, variation in frequency range,

incomplete reporting of sample thickness, and omission of fitting residuals produce non-comparable conductivity values across studies (Kanimozhi, 2022). High-quality reports explicitly disclose electrode type, geometry, fitting model, and conditioning protocol, thereby enabling reproducible parameter extraction and cross-study comparison.

#### Methanol Permeability and Device-Level Considerations

In direct methanol fuel cells (DMFCs), methanol crossover is a key performance parameter. Functional nanofillers that increase tortuosity and reduce free volume have demonstrated reduced methanol permeability, although this sometimes occurs at the expense of decreased proton conductivity (Pourzare *et al.*, 2016). Device-oriented analyses further reveal that ex-situ conductivity does not directly translate to full-cell performance due to catalyst-layer compatibility, water management, and mass-transport limitations (Jiao *et al.*, 2021).

Comprehensive membrane-electrode assembly (MEA) integration studies remain limited in the proton-conducting nanocomposite literature. Future research must evaluate membrane performance within operational electrochemical cells rather than relying solely on standalone conductivity metrics.

#### 4. Structure–Property Relationship (Critical Synthesis)

The collective body of literature demonstrates that enhanced proton conduction in nanocomposite polymer membranes results from a complex and interdependent interplay of structural and interfacial factors rather than from any single modification strategy. A consistent finding across systems is that reduction in crystallinity and corresponding increase in amorphous phase fraction facilitate ionic mobility by promoting segmental motion of polymer chains (Croce *et al.*, 1999; Tan *et al.*, 2020). This structural softening enhances the availability of free volume and dynamic pathways necessary for proton hopping. Simultaneously, incorporation of inorganic nanofillers can elevate the local dielectric constant at polymer–filler interfaces, thereby enhancing salt dissociation and increasing the effective concentration of mobile charge carriers (Pandey *et al.*, 2011; Hunpratub *et al.*, 2009) [17, 22, 23]. These interfacial regions

often act as preferential conduction zones, particularly when filler surfaces contain hydroxyl or other polar functional groups capable of stabilizing protonic species.

Equally critical is the quality of nanofiller dispersion. Uniform distribution without agglomeration maximizes interfacial area and maintains polymer chain flexibility, whereas clustering introduces rigidity and tortuosity that can impede proton transport (Al-Sagheer *et al.*, 2023). Maintenance of polymer chain flexibility is essential for sustaining segmental motion–assisted conduction mechanisms, as emphasized in both classical and recent studies (Agrawal *et al.*, 2013) [2]. Thus, the most effective systems balance structural amorphization, efficient salt dissociation, optimized interfacial polarization, and preserved mechanical flexibility.

Despite these general principles, notable contradictions persist in the literature. Certain systems exhibiting strong dielectric enhancement or significant crystallinity suppression display only modest conductivity improvements, whereas others with relatively minor structural modifications report comparatively large transport gains. These inconsistencies are often attributable to non-standardized experimental conditions, particularly humidity control and sample conditioning, as well as incomplete nanoscale dispersion characterization and variability in electrode configuration and impedance fitting protocols (Kanimozhi, 2022; Tan *et al.*, 2020). Such methodological disparities complicate meta-analysis and obscure transferable design rules.

To establish reliable and broadly applicable structure–property relationships for high-performance proton-conducting nanocomposite membranes, future investigations must adopt standardized reporting practices. These include explicit documentation of temperature, relative humidity, and membrane thickness; provision of nanoscale dispersion evidence through TEM and elemental mapping; measurement of ionic transference numbers to differentiate mobility-driven and concentration-driven conductivity enhancements; and full disclosure of electrochemical impedance spectroscopy fitting models, electrode geometry, and residual analysis. Adoption of these practices will enable rigorous cross-study comparison and support the rational design of advanced proton exchange membrane materials.

**Table 1:** Structural–Thermal–Electrical Correlation in Selected Proton Conducting Polymer Electrolytes

| System   | Composition             | Crystallinity (%)        | Tg (°C) | Conductivity (S cm <sup>-1</sup> ) | Temp (°C) | Activation Energy (eV) | Measurement Conditions               | Reference                        |
|--|-------------------------|--------------------------|---------|------------------------------------|-----------|------------------------|--------------------------------------|----------------------------------|
| PVA/Proline  | 75PVA:25Proline         | 12.79                    | 67      | ~1.0 × 10 <sup>-5</sup>            | RT        | —                      | 42 Hz–1 MHz, Al electrodes           | (Hemalatha <i>et al.</i> , 2019) |
| PVA/Proline + NH <sub>4</sub> SCN                              | 0.4 wt% salt            | 10.86                    | 45      | 5.64 × 10 <sup>-4</sup>            | RT        | 0.32                   | 42 Hz–1 MHz, Al electrodes           | (Hemalatha <i>et al.</i> , 2019) |
| PVA/Proline + NH <sub>4</sub> SCN (Optimal)                    | 0.5 wt% salt            | 9.19                     | 42      | 1.17 × 10 <sup>-3</sup>            | RT        | 0.21                   | 42 Hz–1 MHz, Al electrodes           | (Hemalatha <i>et al.</i> , 2019) |
| PVA/Proline + NH <sub>4</sub> SCN                              | 0.6 wt% salt            | 23.15                    | 54      | 3.45 × 10 <sup>-4</sup>            | RT        | 0.38                   | 42 Hz–1 MHz                          | (Hemalatha <i>et al.</i> , 2019) |
| PVA–NH <sub>4</sub> CH <sub>3</sub> COO                        | No filler               | —                        | —       | 2.36 × 10 <sup>-5</sup>            | 30        | 0.41                   | 1 Hz–1 MHz, Pt electrodes            | (Ranjta <i>et al.</i> , 2021)    |
| PVA–NH <sub>4</sub> CH <sub>3</sub> COO + BiNiFeO <sub>3</sub> | 0.4 wt% filler          | -                        | —       | 8.72 × 10 <sup>-5</sup>            | 30        | 0.28                   | 1 Hz–1 MHz, Pt electrodes            | (Ranjta <i>et al.</i> , 2021)    |
| PEO–LiClO <sub>4</sub>   | Control (no filler)     | Semi-crystalline         | —       | ~1.0 × 10 <sup>-6</sup>            | 30        | —                      | 1 MHz–0.1 Hz, SS blocking electrodes | (Tan <i>et al.</i> , 2020)       |
| PEO–LiClO <sub>4</sub> –SiO <sub>2</sub>                       | 10 wt% SiO <sub>2</sub> | Suppressed crystallinity | —       | 1.1 × 10 <sup>-4</sup>             | 30        | 0.24                   | 1 MHz–0.1 Hz, SS electrodes          | (Tan <i>et al.</i> , 2020)       |
| PVA:MC:NH <sub>4</sub> Cl                                      | 50 wt%                  | —                        | —       | 1.99 × 10 <sup>-3</sup>            | RT        | -                      | 50 Hz–5000 kHz SS electrodes         | (Aziz <i>et al.</i> , 2022)      |

**Table 2:** Electrochemical and Conductivity Performance vs Filler Loading

| System   | Filler Loading | Ionic Conductivity (S cm <sup>-1</sup> ) | Temperature | Activation Energy (eV) | Electrochemical Stability Window (V) | Electrode Type | Key Observation                    | Reference                        |
|--|----------------|--|-------------|------------------------|--------------------------------------|----------------|------------------------------------|----------------------------------|
| PVA–NH <sub>4</sub> CH <sub>3</sub> COO                        | 0 wt%          | 2.36 × 10 <sup>-5</sup>                  | 30 °C       | 0.41                   | ±3.2 V                               | Pt             | Baseline gel system                | (Ranjta <i>et al.</i> , 2021)    |
| PVA–NH <sub>4</sub> CH <sub>3</sub> COO + BiNiFeO <sub>3</sub> | 0.2 wt%        | 5.14 × 10 <sup>-5</sup>                  | 30 °C       | 0.35                   | —                                    | Pt             | Conductivity increases with filler | (Ranjta <i>et al.</i> , 2021)    |
| PVA–NH <sub>4</sub> CH <sub>3</sub> COO + BiNiFeO <sub>3</sub> | 0.4 wt%        | 8.72 × 10 <sup>-5</sup>                  | 30 °C       | 0.28                   | ±4.68 V                              | Pt             | Optimal loading; reduced Rb        | (Ranjta <i>et al.</i> , 2021)    |
| PVA–NH <sub>4</sub> CH <sub>3</sub> COO + BiNiFeO <sub>3</sub> | 0.8 wt%        | 4.91 × 10 <sup>-5</sup>                  | 30 °C       | 0.39                   | —                                    | Pt             | Agglomeration reduces σ            | (Ranjta <i>et al.</i> , 2021)    |
| PVA/Proline/NH <sub>4</sub> SCN                                | 0.5 wt%        | 1.17 × 10 <sup>-3</sup>                  | RT          | 0.21                   | 3.61 V                               | SS blocking    | Highest σ; lowest crystallinity    | (Hemalatha <i>et al.</i> , 2019) |
| PEO–LiClO <sub>4</sub> –SiO <sub>2</sub> (in-situ)             | 10 wt%         | 1.1 × 10 <sup>-4</sup>                   | 30 °C       | 0.24                   | 5.0 V (vs Li/Li <sup>+</sup> )       | SS/Li          | Stable 700 h cycling               | (Tan <i>et al.</i> , 2020)       |
| PVA:MC:NH <sub>4</sub> Cl                                      | 50 wt%         | 1.99 × 10 <sup>-3</sup>                  | RT          | -                      | 1.4 V                                | SS             | Highest σ; EDLC compatible         | (Aziz <i>et al.</i> , 2022)      |

## References

- Agrawal SL, Pandey K. Electrical and electrochemical properties of proton conducting polymer electrolytes. *Journal of Electroceramics*,2010;25(2):99–108.
- Agrawal SL, Rai N, Chand N. Ion transport and dielectric behavior of nanocomposite polymer electrolytes. *Ionics*,2013;19(1):145–156.
- Appetecchi GB, Scrosati B, Zane D. Composite polymer electrolytes for lithium batteries. *Journal of The Electrochemical Society*,2004;151(9):A1369–A1374.
- Aranda P, Ruiz Hitzky E. Polymer nanocomposites as new materials. *Chemistry of Materials*,1992;4(6):1395–1403.
- Armand MB, Chabagno JM, Duclot M. Polymer solid electrolytes. In *Proceedings of the Second International Meeting on Solid Electrolytes*, 2015, 131–136.
- Bansal AK, Dissanayake MAK. Ionic transport in polymer electrolytes. *Ionics*,2000;6(3–4):239–246.
- Bharathi KR, Chandramohan A, Sekhar JC, Kandhaswamy MA. Structural studies of ferrite based materials. *Crystal Research and Technology*,2007;42(6):595–601.
- Bhide A, Hariharan K. Ionic transport studies on proton conducting polymer electrolytes. *Polymer International*,2008;57(4):523–529.
- Chandra S. *Superionic solids principles and applications*, 1981.
- Chau KH, Wong YW, Shin FG. Electrical properties of composite polymer electrolytes. *Applied Physics Letters*,2009;94(20):202902.
- Croce F, Appetecchi GB, Persi L, Scrosati B. Nanocomposite polymer electrolytes for lithium batteries. *Nature*,1998;394(6692):456–458.
- Deepa M, Awadhia A, Bhandari S, Agrawal SL. Structural and electrical properties of polymer electrolytes. *Electrochimica Acta*,2008;53(24):7266–7274.
- Dias FB, Plempl L, Veldhuis JB. Polymer electrolytes for electrochemical devices. *Journal of Power Sources*,2000;88(2):169–191.
- Dwivedi MM, Asthana N, Pandey K. Nanocomposite polymer electrolytes for energy devices. *Open Journal of Chemical Engineering and Science*,2014;1(1):26–33.
- Fenton DE, Parker JM, Wright PV. Complexes of alkalimetal ions with polyethers. *Polymer*,1973;14(11):589–594.
- Gray FM. *Solid polymer electrolytes fundamentals and technological applications*, 1991.
- Hunpratub S, Thongbai P, Yamwong T, Yimnirun R, Maensiri S. Dielectric properties of bismuth ferrite ceramics. *Applied Physics Letters*,2009;94(6):062904.
- Kremer F, Schönhals A. *Broadband dielectric spectroscopy*, 2003.
- Liang CC. Conduction characteristics of composite electrolytes. *Journal of The Electrochemical Society*,1973;120(10):1289–1292.
- MacCallum JR, Vincent CA. *Polymer electrolyte reviews*, 1987, 1–2.
- Mellander BE, Albinsson I. Ionic conductivity in polymer electrolytes. In *Solid state ionics new developments*, 2015, 97–110.
- Pandey K, Dwivedi MM, Singh M, Agrawal SL. Multiferroic filler based nanocomposite polymer electrolytes. *Phase Transitions*,2011;84(4):343–356.
- Pandey K, Singh M, Asthana N, Dwivedi MM, Agrawal SL. Electrical behavior of nanocomposite polymer electrolytes. *International Journal of Materials Science*,2011;1(2):9–18.
- Passerini S, Scrosati B, Appetecchi GB. Polymer electrolytes for lithium and proton batteries. *Journal of Power Sources*,2000;88(2):169–177.
- Pinnavaia TJ, Bell GW. *Polymer clay nanocomposites*, 2000.
- Rittidech A, Porkornwong N, Suthapintu A. Ferroelectric fillers in polymer electrolyte systems. *Ferroelectrics*,2009;382(1):62–71.
- Scrosati B. Applications of electroactive polymers, 1993.
- Scrosati B, Garche J. Lithium batteries status and perspectives. *Journal of Power Sources*,2010;195(9):2419–2430.
- Sekhon SS, Arora N, Singh HP. Proton conducting polymer electrolytes. *Solid State Ionics*,2003;160(3–4):301–308.
- Shen Y. Cognitive constraints on directionality in semantic structures. *Poetics*,1995;23(4):255–274.
- Shuttleworth S. *The mind of the child*, 2010.
- Sontag S. *Illness as metaphor*, 1978.
- Sun X, Kerr JB, Angell CA. Conductivity and dynamics of polymer electrolytes. *Electrochimica Acta*,1998;43(10–11):1327–1334.
- Vincent CA. *Polymer electrolyte fundamentals*. *Progress in Solid State Chemistry*,1987;17(3):145–261.

35. Weston J, Steele BCH. Effects of inert fillers on polymer electrolytes. *Solid State Ionics*, 1982;7(2):75–79.
36. Wieczorek W. Composite polyether based electrolytes, 1995.
37. Wright PV. Electrical conductivity in polymer electrolytes. *British Polymer Journal*, 1975;7(5):319–327.
38. Xue Z, He D, Xie X. Polyethylene oxide based electrolytes for lithium ion batteries. *Journal of Materials Chemistry A*, 2015;3(38):19218–19253.
39. Yang S, Liu Z, Wang Y. Nanocomposite polymer electrolytes for energy storage. *Electrochimica Acta*, 2014;146:649–656.
40. Zunshine L. *Why we read fiction theory of mind and the novel*, 2006.